A DETERMINATION OF L SHELL PARTICLE PARAMETERS FOR TRANSITIONS IN THULIUM-169

A THESIS

Presented to

The Faculty of the Division

of Graduate Studies

By

Craig McKinney Hill

In Partial Fulfillment

of the Requirements for the Degree

Doctor of Philosophy

in the School of Physics

Georgia Institute of Technology

May, 1975

A DETERMINATION OF L SHELL PARTICLE PARAMETERS

FOR TRANSITIONS IN THULIUM-169

Approved:

E. T. Patronis, Jr., Chairman

C. H. Braden

C. J. Roberts

Date approved by Chairman: 27 May 75

ACKNOWLEDGMENTS

To my thesis advisor, Dr. E. T. Patronis, Jr., I extend my appreciation for guidance and assistance throughout this project. Dr. L. D. Wyly, Jr., was helpful in many ways, and most generous with his time. Professor N. S. Kendrick brought the computer back to life more than once.

Dr. C. H. Braden and Dr. C. J. Roberts served conscientiously as members of the reading committee, Mr. K. B. Springfield and Mr. J. T. Callahan skillfully constructed parts of the mechanical apparatus, and Dr. D. A. McClure provided one of the germanium detectors used in the experiments. Dr. M. E. McLain and Mr. R. C. McFarland were most accommodating in having the sources irradiated and chemically processed. Financial assistance was provided by a three-year NDEA fellowship.

To my parents, Mr. and Mrs. Francis M. Hill, go my sincere thanks and deep appreciation for their sustaining encouragement throughout these years.

TABLE OF CONTENTS

Appendix Page

LIST OF TABLES

LIST OF ILLUSTRATIONS

SUMMARY

The low-lying states of Tm^{169} which are populated following electron capture decay of Yb^{169} have been studied extensively, as have the electromagnetic transitions from these levels. Gamma-gamma and K electron-gamma directional correlation measurements have been performed on Tm^{169}, from which K shell electron particle parameters have been deduced.

The present research was undertaken in order to determine the L shell particle parameters for certain of the decay transitions in Tm^{169}. Directional correlations between L conversion electrons and gamma rays were observed for the 198 keV/110 keV and the 177 keV/130.5 keV cascades. The gamma-gamma directional correlations for these cascades were also observed.

The experimental arrangement included radiation detectors, electronic fast-slow coincidence circuitry, and an on-line digital computer. A solid-state Si(Li) diode (12.5 mm diameter X 2 mm nominal sensitive depth) was used for detection of the electrons. Two Ge(Li) detectors were employed in the course of the experiments, with approximate active volumes of 25 cm^3 and 30 cm^3. The energy resolution of the Si(Li) detector was about 6.1 keV FWHM at the energies encountered here. Both the Ge(Li) detectors were able to cleanly separate the desired gamma lines from unwanted

radiations. The computer was used to control the routine aspects of the experiments, and to collect and store the data.

Particle parameters were introduced in theoretical work in order to describe the directional correlation between particle radiations in terms of the corresponding gamma-gamma directional correlation. Experimentally, the electron particle parameter b_k for a transition is defined as

$$b_k = \frac{A_{kk}(e,\gamma)}{A_{kk}(\gamma,\gamma)} ,$$

where $A_{kk}(e,\gamma)$ and $A_{kk}(\gamma,\gamma)$ are the electron-gamma and the gamma-gamma directional correlation coefficients (of order k), respectively. In most cases of interest, k = 2 or k = 4. The L shell particle parameters measured here are weighted sums of the particle parameters for the individual L subshells and for the two multipolarities which contributed to each converted transition observed.

The gamma-gamma correlation measurements, which were performed using the two Ge(Li) detectors, yielded $A_{22}(198, 110) = 0.320\pm0.006$ and $A_{22}(177,130.5) = 0.257\pm0.007$.

Electron L shell particle parameters for k = 2 were obtained for the 198 keV, 177 keV, and 110 keV transitions in Tm^{169}. For the first of these, the result $b_2 = 0.331\pm0.038$ was found. The theoretically calculated value is 0.358, using

the E2/M1 mixing ratio indicated by L subshell conversion intensity ratios. Thus, the experimental and theoretical values for b_2^L(198 keV) are in agreement.

For the 177 keV transition, the value $b_2^L = -0.027 \pm 0.045$ was obtained. The theoretical value is 0.093. This discrepancy is somewhat unexpected in view of the substantial agreement for the 198 keV transition. However, the halflife of the 139 keV level (the intermediate state for the 177 keV/130.5 keV cascade) is about four times as long as the halflife of the 118 keV level (the intermediate state for the 198 keV/110 keV cascade). Moreover, the magnetic dipole moment for the 139 keV is greater than the magnetic moment of the 118 keV level by a factor of roughly 1.8. Thus, $(\mu\tau)_{139} \approx 8\times(\mu\tau)_{118}$. It may be possible that a hyperfine interaction between the Tm^{169} nucleus at the 139 keV level and the disrupted electron shell (following the first transition, which was converted) is sufficient to considerably affect the $177e_L/130.5\gamma$ correlation, whereas the same type of interaction might not be able to affect the $198e_L/110\gamma$ correlation to nearly the same extent.

For the 110 keV transition, the b_2^L value found was -0.037 ± 0.036. The theoretically predicted value is 0.179. The cascade used in the measurement of b_2(110 keV) was the same one as used in the measurement of b_2(198 keV), and furthermore the first transition was not converted in this case. Presumably then, a hyperfine interaction between the

nucleus and the electron shell would not be responsible for the difference between the experimental and theoretical values. The kinetic energy of the converted L electrons for this transition is about 100 keV, which is a relatively low energy. So in this case, it may be that electron scattering in the source had a significant effect on the correlation.

CHAPTER I

INTRODUCTION

The two most frequently encountered processes of decay of excited nuclear states are gamma ray emission and internal conversion. Both are electromagnetic interactions which involve the removal of energy from an atomic nucleus. In the first case the energy appears as a quantum (gamma ray photon) of the electromagnetic field, in the second instance the energy is transferred directly to an orbital electron by expelling it from the atom. It may happen that a given excited nuclear state can decay by both of these processes. The relative probability of internal conversion vis-a-vis gamma emission is defined to be the "internal conversion coefficient," α.

The probability that a nucleus in an excited state will emit a de-excitation radiation will depend, in general, on the orientation of the nuclear spin axis with respect to the direction of emission. Ordinarily, the spin axes of nuclei in a sample will be randomly oriented, and the intensity pattern of radiation from such nuclei will be isotropic. However, if a subset of nuclei preferentially oriented with respect to a certain fixed direction can be selected, then the intensity of radiation from this subset may indeed be

correlated with the direction of emission. A nuclide which has excited states depopulated by two successive radiations, R_1 and R_2, offers the possibility of selecting such an ensemble of non-randomly oriented nuclei (1). The detection of the radiation R_1 along only one fixed direction from a point source selects a subset of nuclei whose spin axes are not randomly distributed with respect to that direction, and the probability of detecting the succeeding radiation R_2 may be correlated in angle with the direction of R_1.

The angular correlation between two successive radiations is expressed in terms of the "correlation function," W. If the first radiation is in the fixed direction $\vec{r}_1$, then the relative probability that the second radiation will be emitted into the small solid angle $d\Omega$ at an angle θ with respect to $\vec{r}_1$ is $W(\theta)\ d\Omega$.

In a typical case, a nuclide would have states A, B, and C in order of decreasing energy, and corresponding angular moments J_A, J_B, and J_C. The radiation R_1 would arise from decays of state A to state B, and R_2 would be due to subsequent decays of state B to state C. The correlation function can be written in the form

$$W(\theta) = \sum_{k=o}^{N} A_{kk}(R_1,R_2)\ P_k(\cos(\theta)). \qquad (I\text{-}1)$$

P_k is the Legendre polynomial, and $A_{kk}(R_1,R_2)$ the angular correlation coefficient, of order k. $N = \min(2J_B, 2L_1, 2L_2)$,

where L_1 and L_2 are the angular momenta of the radiations R_1 and R_2, respectively. The usual convention, which will be followed here, is to choose $A_{00} = 1$. If the polarizations of the radiations R_1 and R_2 are not observed, then the index "k" in equation (I-1) is further restricted to be an even integer. In the literature the term "directional correlation" is applied to experiments in which the polarizations are not determined, which is the case in the present investigation.

Each correlation coefficient, $A_{kk}(R_1,R_2)$, can be written as a product of two partial correlation coefficients, $A_k(R_1)$ and $A_k(R_2)$, each of which depends on only one transition of the cascade. It is shown in Appendix A that a partial gamma correlation coefficient for a transition of mixed multipolarity, L and L+1, and (gamma) mixing ratio, δ, can be expressed in the form

$$A_k(\gamma) = [F_k(L,L,J,J_B) + 2\delta F_k(L,L+1,J,J_B) + \delta^2 F_k(L+1,L+1,J,J_B)]\ (1+\delta^2)^{-1}. \qquad \text{(I-2)}$$

Here, J denotes either J_A or J_C, depending on whether the gamma-radiation is R_1 or R_2, in our previous terminology. Each F function depends only on the nuclear spins, the radiation multipolarities, and the index k.

The gamma-gamma correlation has been adopted as the

standard, and other types are expressed as modifications thereto, via the so-called "particle parameters," which are defined in Appendix A. The particle parameters for electron-gamma correlations will depend on the multipolarity, parity, and energy of the transition, and on the atomic number of the emitting nuclide. In some cases the parameters may depend significantly on nuclear structure also. Referring again to Appendix A, we see that the partial correlation coefficient for a converted transition can be written as

$$A_k(e) = [b_k(L,L)\cdot F_k(L,L,J,J_B) + 2\delta_e\cdot b_k(L,L+1)\cdot F_k(L,L+1,J,J_B) + \delta_e^2\cdot b_k(L+1,L+1)\cdot F_k(L+1,L+1,J,J_B)]\cdot (1+\delta_e^2)^{-1}. \qquad (I-3)$$

The L's and J's are as previously defined, the b_k's are the particle parameters (which also depend on the shell, or subshell, from which conversion takes place), and $\delta_e = \delta(\alpha_{L+1}/\alpha_L)^{1/2}$, where α_L and α_{L+1} are the partial conversion coefficients for the transition.

Comparing equations (I-2) and (I-3), we see that the ratio $A_{kk}(e,\gamma)/A_{kk}(\gamma,\gamma)$ yields a particle parameter directly, if $\delta = 0$ for the converted transition which was observed. If $\delta \neq 0$ for that transition, then the ratio of correlation coefficients is not simply a particle parameter, but instead

is a weighted sum of them.

Experimental Procedure

A directional correlation experiment is performed by using two detectors, D_1 (fixed) and D_2 (moveable), with D_1 electronically gated on radiation R_1 and D_2 gated on R_2. The radioactive source (ideally a point) is placed at the intersection of the axes of the detectors (each assumed to be cylindrically symmetric). An electronic system is set to record a count if a radiation of type R_2 is detected by D_2 within a certain small time interval ("resolving time") of detection of a radiation of type R_1 by detector D_1. D_2 is then positioned at various angles with respect to D_1 in a plane, and the coincidence counting rate is recorded at each of these angles. The resolving time of the system allows some nearly simultaneous radiations from different nuclei to be recorded as coincidence counts from one nucleus, and the spatial extension of the detectors makes the recorded correlation an average of the true one over the angles subtended by the detectors as seen from the source. Also, if the source is large enough, additional deviations will be introduced into the observed correlation. After corrections for these effects have been included, the true correlation in angle between the two radiations can be computed.

Attenuation Mechanisms

Thus far, the discussion has assumed that the state

of the nucleus remains undistrubed during the time between the first and second transitions of a cascade decay. The directional correlation between two successive radiations can be altered or destroyed if the orientation of the nuclear spin axis is changed during the intermediate state. Interactions of the nuclear magnetic dipole moment or electric quadrupole moment with extra-nuclear magnetic fields or electric field gradients, respectively, or a hyperfine interaction between the nucleus and its electronic shell, are possible sources of nuclear reorientation during the intermediate state. Whether such interactions will affect the correlation in a particular case depends on the strength of the interaction and the lifetime of the intermediate state.

For interactions of the nucleus with statistically isotropic static fields or gradients, as in a microcrystalline powder source, the form of the correlation function is unaltered, but each original correlation coefficient will be multiplied by an attenuation factor (1). In such a case, the ratio $A_{kk}(e,\gamma)/A_{kk}(\gamma,\gamma)$ will be unchanged if the interaction is the same for both the gamma-gamma and the electron-gamma correlation.

Two mechanisms which may affect an electron-gamma correlation but not the corresponding gamma-gamma correlation are (i) electron scattering, and (ii) interaction of the nucleus with the disrupted electron shell, if the first

transition of the cascade is converted. The experimental procedure to be followed in minimizing electron scattering is to use a thin radioactive source, thin backing material of low atomic number, and to have an evacuated path between the radioactive source and electron detector. The severity of scattering will depend on the electron kinetic energy, being more important at low than at high energies.

Historical Development of Directional Correlations

The first theoretical treatment of angular correlations between successive nuclear radiations was that of D. R. Hamilton (2) in 1940. This was restricted to gamma-gamma correlations. Since then, the theory has been greatly extended and refined. Comprehensive review expositions of general angular correlations have been given by L. C. Biedenharn and M. E. Rose (3), by Biedenharn (4), and by H. J. Rose and D. M. Brink (5).

The first successful gamma-gamma directional correlation experiment was carried out by Brady and Deutsch (6) in 1947, using Geiger counters. The subsequent introduction of scintillation detectors, higher-speed electronic coincidence circuitry, and multichannel pulse height analyzers into this work greatly extended the range of applicability of the technique and drastically reduced the time necessary to perform a given experiment. Solid-state germanium diode detectors, which have a very superior gamma

ray energy resolution as compared to scintillation counters, have come into widespread use since the early 1960's.

Several projects for the calculation of particle parameters have been carried out since interest first arose in directional correlations involving conversion electrons. The different calculations have been at various levels of sophistication and refinement. The theoretical particle parameters used in this study are those of Hager and Seltzer (7). They obtained the electron wavefunctions by a relativistic self-consistent-field calculation, and took into account the finite size of the nucleus. Further details on their method, and references to and comments on previous particle parameter calculations of other workers, can be found in references (7) and (8).

Purpose of the Research

The purpose of this research is to determine L-shell directional correlation particle parameters of the 110, 177, and 198 keV transitions in the nuclide Tm^{169}, and to make a measurement of the gamma-gamma directional correlation coefficients of the 198 keV/110 keV and 177 keV/130.5 keV cascades with a spectrometer system capable of resolving the desired gamma radiations from interfering ones.

Review of Previous Research on Tm^{169}

The level structure and decay scheme of Tm^{169} relevant to this investigation are shown in Figure 1.

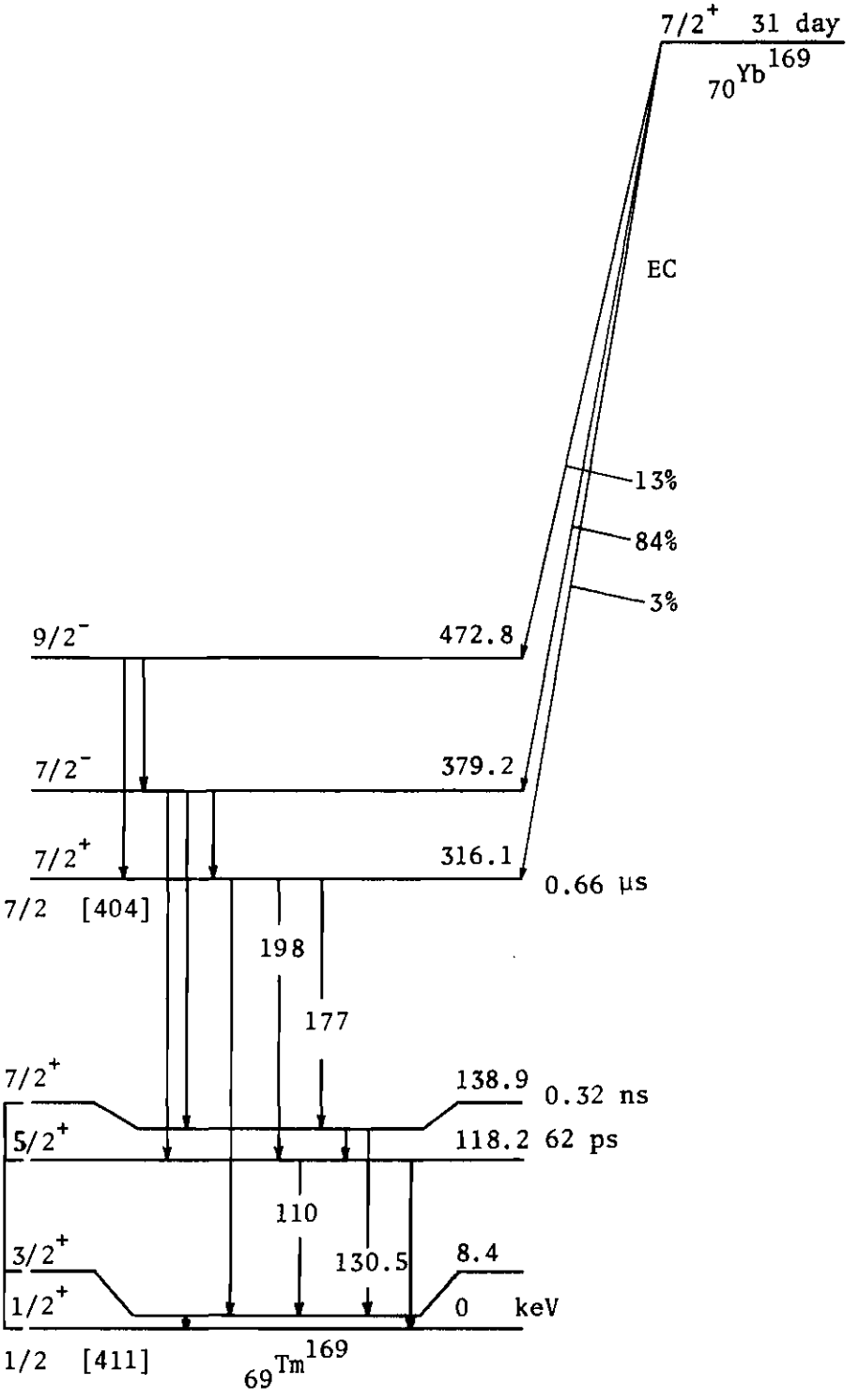

Figure 1. Relevant Features of Tm^{169} De-excitation Scheme Following Electron Capture Decay of Yb^{169}

Johansson (9) was the first to deduce the main features of this scheme, and other studies were made subsequently (10), (11), (12). A theoretical interpretation of Tm^{169} in terms of the "unified model" of nuclear structure is given in references (9) and (13).

The halflife of the 118 keV level was found to be 62±3 picoseconds by Blaugrund et al. (14), and the magnetic dipole moment of this level has been calculated (17) from data presented by Gunther et al. (15) to be 0.72±0.08 nuclear magneton.

Sundstrom et al. (16) determined the halflife of the 139 keV level to be 321±14 picoseconds by a delayed coincidence measurement, and calculations (17) using data given by Gunther et al. (15) give the magnetic dipole moment of this level as 1.30±0.07 nuclear magnetons.

Gamma ray mixing ratios for the 110, 177, and 198 keV transitions have been calculated (17) from L-subshell conversion electron intensity ratios, giving $|\delta_{110}(E2/M1)|$ = 0.152±0.007, $|\delta_{177}(E2/M1)|$ = 0.44±0.02, and $|\delta_{198}(E2/M1)|$ = 0.332±0.016. L-subshell ratios are consistent with the assignment of pure E2 multipolarity to the 130.5 keV transition (17).

Numerous gamma-gamma directional correlation experiments have been performed on the 198 keV/110 keV cascade (15,18-23), and on the 177 keV/130.5 keV cascade (18-21, 23-25). Most of these measurements were made using two

NaI(Tl) gamma detectors, or one NaI(Tl) and one Ge(Li) detector.

Grabowski et al. (19) measured the 198 keV/(110&118) keV, K conversion electron-gamma directional correlation, using a magnetic spectrometer for selection of the electrons and NaI(Tl) for detection of the gamma radiation. They obtained $A_{22}(e_K,\gamma) = 0.001\pm0.008$. This value, together with their result of $A_{22}(\gamma,\gamma) = 0.295\pm0.007$ for the same cascade, gives $A_{22}(e_K,\gamma)/A_{22}(\gamma,\gamma) = 0.003\pm0.028$. Agnihotry et al. (25) obtained results for the same K electron gamma correlation which yield $A_{22}(e_K,\gamma)/A_{22}(\gamma,\gamma) = 0.193\pm0.035$. The theoretical prediction (7) for this quantity is 0.134 ± 0.003, assuming the previously quoted mixing ratio for this transition.

Grabowski et al. (19) also measured the 198 keV/ 110 keV, gamma-K electron, directional correlation and their results give $A_{22}(\gamma,e_K)/A_{22}(\gamma,\gamma) = -0.017\pm0.021$. The theoretical prediction (7) is $A_{22}(\gamma,e_K)/A_{22}(\gamma,\gamma) = -0.029\pm 0.001$.

The 177 keV/130.5 keV, gamma-gamma and gamma-K conversion electron, directional correlations were measured by Grabowski et al. (19) and by Agnihotry et al. (25). Values of $A_{22}(\gamma,e_K)/A_{22}(\gamma,\gamma)$ obtained from their results are 1.81 ± 0.08 and 1.84 ± 0.08, respectively. These are in good agreement with the theoretical prediction (7) of $b_2^K(130.5\text{ keV}) = 1.848$ for a pure E2 transition.

Additional information on Tm^{169} and extensive references to the literature on this nuclide may be found in references (17) and (26).

CHAPTER II

EXPERIMENTAL APPARATUS

The directional correlation spectrometer system used in this investigation was composed of: radiation detectors; a vacuum system which enclosed the source and electron detector, when measuring electron-gamma correlations; electronic amplifiers, pulse shapers, pulse height analyzers, and coincidence circuits; data recording equipment; a turntable to position the moveable detector at different angles; and a computer to control the routine aspects of the experiments. These various components will be described in more detail below.

Radiation Detectors

The two gamma ray detectors used in this investigation were solid-state lithium-drifted germanium (Ge(Li)) diodes. One of these, which was employed as the moveable detector, was a Nuclear Diodes Inc. model LGC 3.5X. Trapezoidal in cross-section, this detector was lithium-drifted on the four sides and on one end. Its nominal active volume was 30 cm^3. The detector was cooled by a copper "cold finger" in contact with liquid nitrogen, and was mounted on top of a dewar. The diode was operated at a reverse bias of 1200 V. The energy resolution of this

detector and its associated electronic system was about 3.4 keV FWHM (full width at half maximum) for incident gamma radiation in the energy range from 100 keV to 200 keV.

The other GE(Li) detector used was a model 8101-0421 manufactured by ORTEC, Inc. This cylindrical detector was lithium-drifted around the lateral surface, and had an active volume of approximately 25 cm^3. This detector also was cooled by a liquid nitrogen cryostat system, and was operated at a reverse bias of about 2000 V. Its energy resolution was about 2.1 keV FWHM, for gamma rays of energy 1.33 MeV.

The electron detector used was a lithium-drifted silicon (Si(Li)) type, manufactured by Kevex Corporation. The area of the exposed face of this circular detector was about 1.2 cm^2, and the radiation sensitive depth was 2 mm, nominally. The reverse bias potential used was 200 V. This type of detector can be operated at room temperature, but in order to increase its energy resolution it was used in conjunction with a thermo-electric cooler (Westinghouse type 816-J). The Si(Li) detector was cemented to the low-temperature end of the cooler, and the high-temperature end of the cooler was coated with high-viscosity silicone grease and pressed firmly into contact with the thick brass support-plate of the vacuum assembly. Copper cooling-coils were soldered to the underside of the brass plate, and water at about 15°C was run through the coils. The thermo-electric

cooler was operated at a current of approximately 20 amperes. The energy resolution of the detector when used with this cooling system, about 6.1 keV FWHM for electrons in the energy range from 100 deV to 200 keV, showed a noticeable improvement as compared to the resolution when operated at room temperature.

A different approach to increasing the Si(Li) detector's resolution was to connect the aluminum fin of the cooler (to which the detector was cemented) with a stainless steel dewar filled with liquid nitrogen, by means of metal braid straps. However, the energy resolution using this method was no better than that obtained with the preceding one; and since this second method was far less convenient to use, it was discarded in favor of the aforementioned one.

Vacuum Assembly

For the measurements of electron-gamma directional correlations, it was necessary to provide an evacuated path between the radioactive source and electron detector in order to prevent scattering of the electrons by gas molecules of the air.

The Si(Li) detector was mounted on the brass support-plate, and the source was attached to a positioner which allowed for adjustment along two horizontal axes. The source-positioner was cemented to the brass support-plate, a few centimeters from the Si(Li) detector. An aluminum cylinder

vacuum housing (~12.4 cm inside diameter, and ~11.7 cm height), with a brass covering-plate at one end, was placed over the source and electron detector. The bottom end of the cylinder fit over a rubber O-ring around the periphery of the support-plate. Rubber vacuum hose connected an electrically driven vacuum pump with a port in the center of the support-plate. A thermocouple vacuum gauge was used to monitor the residual pressure of the vacuum chamber. Under operating conditions, this pressure was less than 30 μm of Hg.

Signals from the Si(Li) detector were transmitted to the preamplifier through a vacuum-sealed port in the support-plate.

The gamma detector was situated outside the vacuum housing, and any gamma radiation detected had first to pass through the 0.8 mm wall of the aluminum cylinder.

Electronics

The basic configuration of the electronic instrumentation used as part of the directional correlation spectrometer system is shown in Figure 2.

The signal pulse height from any of the detectors used was very nearly proportional to the energy deposited in the detector by the incident radiation. Signals from each detector were amplified and shaped so as to be bipolar. The outputs of each amplifier were connected to both a

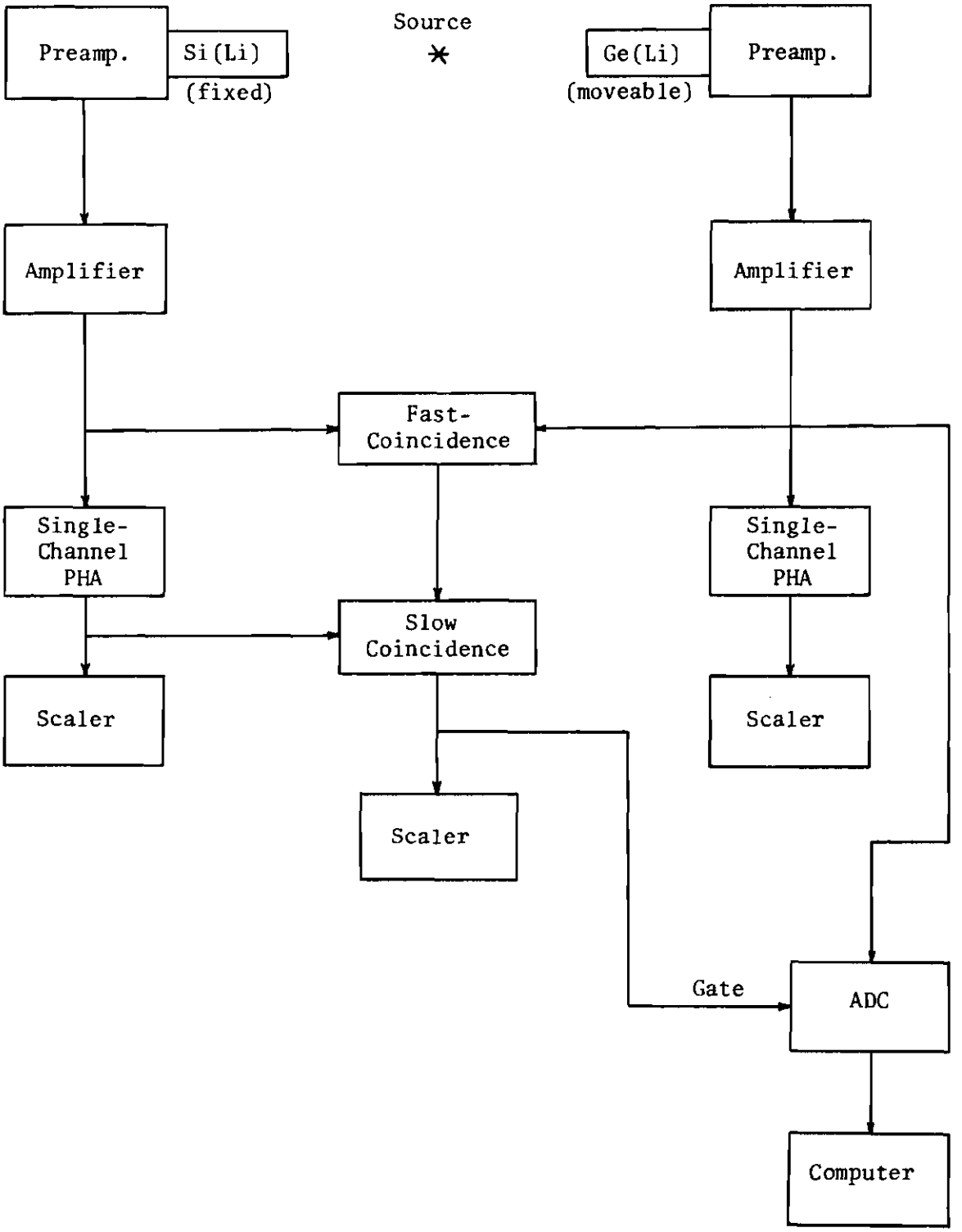

Figure 2. Block Diagram of Electronic Instrumentation as Used for Electron-Gamma Correlations

fast-coincidence circuit and a single-channel pulse height analyzer. The fast-coincidence circuit derived narrow timing pulses from the zero cross-over of the bipolar signals furnished by the amplifier. The width of these narrow pulses determined the resolving time of the system. In these experiments, 2τ was approximately 50 nanoseconds. If two such pulses, one from each half of the circuit, overlap in time then the fast-coincidence circuit sends an output signal to the slow-coincidence circuit. The single-channel analyzer following the electron detector was adjusted to give an output pulse only if the input pulse was in a certain height range, corresponding to the particular conversion line desired. If the slow-coincidence circuit received simultaneous signals from the electron single-channel analyzer and the fast-coincidence circuit, then it in turn sent an output pulse ("gate") to the ADC (analog-to-digital converter). The ADC and part of the computer memory core were used as a multichannel pulse height analyzer. When gated, the ADC increased by one unit the count in the core memory location corresponding to the height of the pulse from the gamma detector.

The fast-coincidence circuit contained variable electronic delays which allowed the signals from the two detectors to be "time aligned." Provision for such alignment is necessary since the signal transmit times for the two branches may not be equal. In addition, a 1/2-microsecond

delay line could be switched into either input of this circuit, to eliminate real coincidences, when measuring the accidental coincidence rate.

When measuring gamma-gamma correlations, the Si(Li) electron detector and its preamplifier were replaced by a Ge(Li) gamma detector and an appropriate preamplifier.

The main amplifiers, the single-channel pulse height analyzers, and the coincidence circuits were designed and built by Dr. E. T. Patronis, Jr. The ADC was a Northern Scientific model NS-625.

Counting Geometry

In each experiment conducted, one radiation detector was moveable and the other detector was stationary. For the electron-gamma correlation experiments, the Si(Li) detector was the stationary one, and for the gamma-gamma experiments the ORTEC Ge(Li) detector was fixed. In each case, the Nuclear Diodes Ge(Li) detector was moveable. This latter detector and its dewar were set on a rotatable aluminum table about 1.5 meters in diameter. The table was connected to a hydraulic motor by a drive belt.

During the course of an experiment, the positioning of the table was under the control of the computer. Manual control was also available for convenience in setting up the experiment. The position of the table was determined electrically by means of a voltage read-off system which

employed a potentiometer whose rotating contact arm was attached to the table. This sensing device and its interface to the computer were designed and constructed by Prof. N. S. Kendrick.

In the experiments, data were taken with angles of 90°, 135°, 180°, 225°, and 270° between the axes of the two detectors.

Computer and Data Collection Program

A Digital Equipment Corporation PDP-8 computer was used on-line to store the coincidence count data, direct the operation of table rotation at the specified times (at intervals of 30 or 60 minutes), and to apply certain acceptability criteria to the fresh batch of data at the end of each counting interval.

The computer system contained three core fields, each of 4096 twelve-bit words, and about 96,000 words on three surfaces of magnetic disk. The DATA program, which controlled the experiments, resided in one field of core, and one surface of magnetic disk was available for permanent storage of data. The remaining core fields and disk memory were available for simultaneous use not connected with the correlation experiments.

The DATA program, which was developed by Dr. C. H. Braden, allowed for an automatic teletype printout of certain useful monitoring information after each counting interval,

and a printout of counting rate for as many as 63 channels could be called for by the teletype operator.

CHAPTER III

DIRECTIONAL CORRELATION MEASUREMENTS

The measurements to be described in this chapter were made in order to determine an experimental directional correlation function, w, of the form

$$w(\theta) = a_0 + a_2 P_2(\cos(\theta)) + a_4 P_4(\cos(\theta)). \qquad \text{(III-1)}$$

The quantity $w(\theta)$ is the experimentally determined coincidence counting rate corresponding to an angle θ between the axes of the two detectors. The coefficients a_0, a_2, and a_4 were obtained by a least-squares fit to the counting rate data, as described in Appendix B. The correlation coefficients A'_{22} and A'_{44} (the primes indicating no correction for solid angle extension) were obtained as $A'_{22} = a_2/a_0$ and $A'_{44} = a_4/a_0$. The geometrically corrected coefficients, A_{22} and A_{44}, of Eq. (I-1) were then found in the manner described in Appendix B. The interpretation of A_{22} and A_{44} for electron-gamma correlations in terms of the electron particle parameters, by means of Eq. (I-3), will be discussed in Chapter IV.

Source Preparation

The stable nuclide Yb^{168} was obtained from Oak Ridge

National Laboratory in the form of Yb_2O_3 powder, enriched to about 18 percent in the ytterbium isotope of mass number 168. An irradiation of this compound by thermal neutrons was carried out at the Georgia Tech Research Reactor, resulting in the production of Yb^{169} by neutron capture. The irradiated oxide was then dissolved in hydrochloric acid, forming water-soluble $YbCl_3$. The acid was removed by evaporation to dryness, and the ytterbium chloride then redissolved in water.

Aluminized mylar film ($\sim$0.8 mg/cm^2) was used as the source backing material. The mylar was glued to a thin aluminum support ring about 3 cm in diameter. A source was prepared by depositing a drop of the concentrated radioactive ytterbium chloride solution onto the mylar film and then allowing it to dry completely. After drying, the source and mylar backing were sprayed with a light coating of acrylic resin in order to prevent flaking of the source material. The diameter of the source was about 5.4 mm. The aluminum source support ring was attached to a source positioner, which in turn was cemented to the brass support-plate of the vacuum housing.

Gamma Ray and Conversion Electron Energy Spectra

Figure 3 shows the low-energy portion of the Tm^{169} gamma ray de-excitation spectrum, obtained with one of the Ge(Li) detectors. The gamma rays of interest here are those

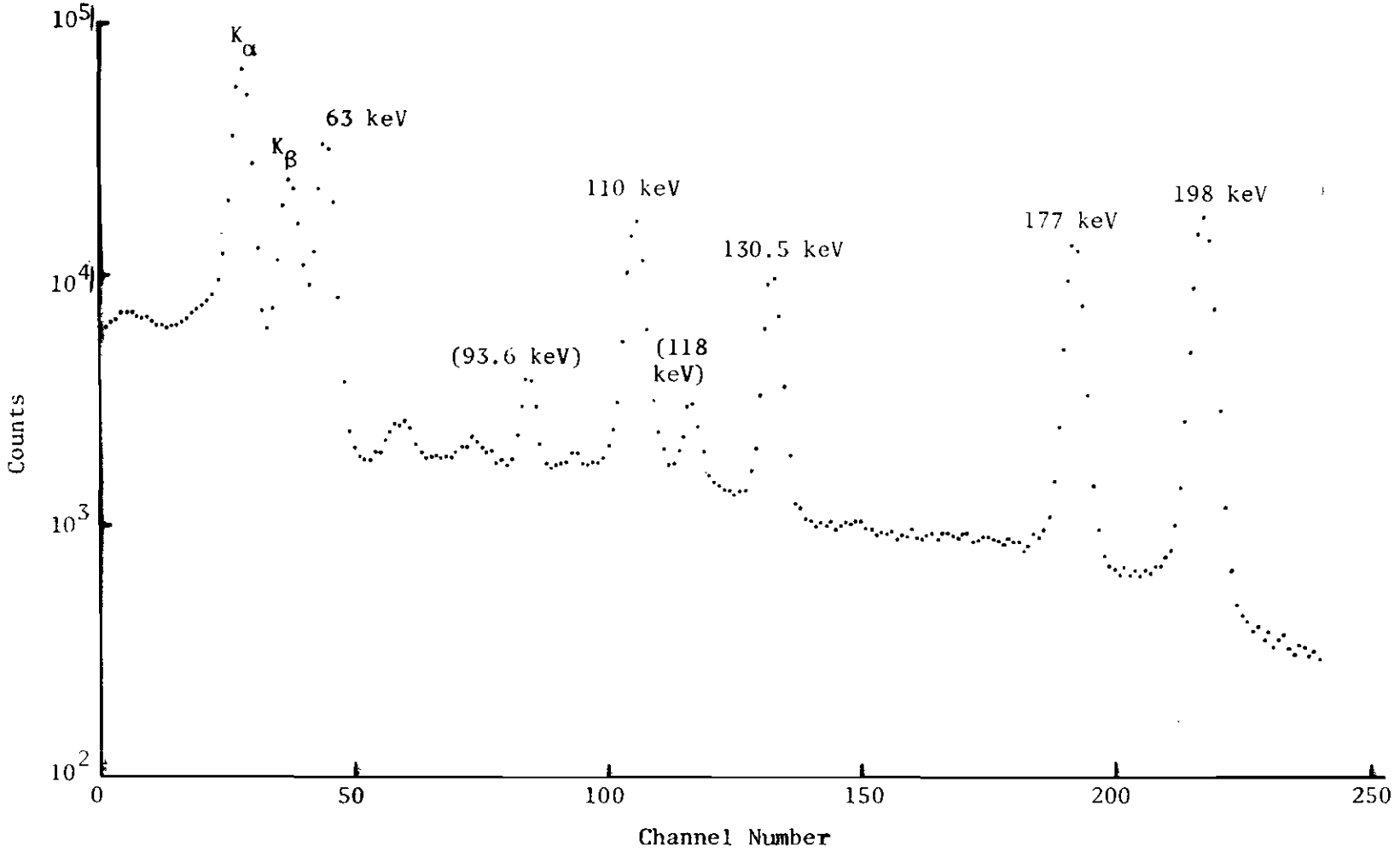

Figure 3. Relevant Portion of Tm^{169} Gamma Ray Spectrum, as Observed by One of the Ge(Li) Detectors

of energy 110, 130.5, 177, and 198 keV.

Figure 4 shows the response of the Si(Li) detector to the Tm^{169} decay radiations. Each line labeled "M" also contains contributions from N and O shell electrons. The energy resolution of the electron detection system was limited by thermal noise generated in the detector and its preamplifier. The noise from the Si(Li) detector was reduced by operating it in conjunction with a thermo-electric cooler, as described in Chapter II. The preamplifier following the Si(Li) detector was a Hewlett Packard model 5554A.

Measurement Procedure

Prior to the start of the experiments, the source was centered by adjusting its position until the counting rates of the moveable detector were as nearly equal as possible at the 90°, 180°, and 270° positions. Generally, these rates were within about 2 percent of each other.

The coincidence time alignment was accomplished in the following manner. Two decay radiations in prompt coincidence with each other were selected, and one of the single-channel analyzers (refer to Figure 2) was adjusted to accept the first of these radiations, while the other analyzer was adjusted to accept the second radiation. A slow-coincidence (i.e., energy) requirement was placed on the outputs of both analyzers, in addition to the fast-coincidence (i.e., time)

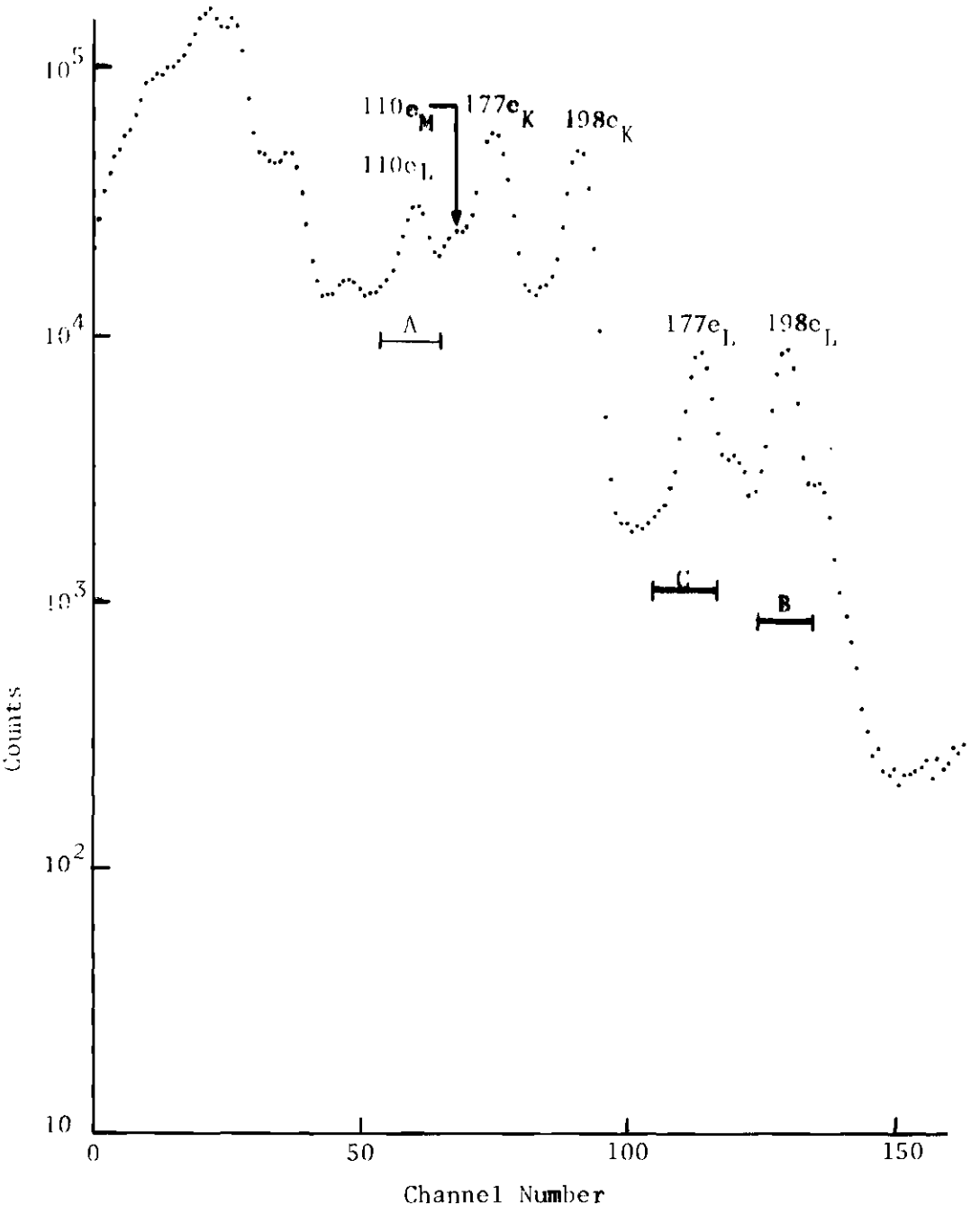

Figure 4. Low-Energy Response of the Si(Li) Detector to the Radiations of Tm^{169}

requirement on the amplifier outputs. The resulting coincidence counting rate was recorded for different time delays in one of the signal branches. The center of the time delay region which gave the highest counting rate was used for the actual experiments, and for these the slow-coincidence requirement was removed from the moveable detector's signal branch.

The experiments were performed by repeated counting at each angle, in a definite sequence, for periods of either 30 or 60 minutes. The longer interval was used in those correlation measurements with lower counting rates. The total counting time for the different correlations varied from two days to two weeks, again depending on the counting rate.

Accidental coincidence counts were taken by switching a 1/2-microsecond time delay into one of the detector signal paths. The accidental rate was presumed to be isotropic with respect to the angle between the two detectors, and the accidental counting rates for all the different angles were automatically combined into one average accidental rate by the computer during the course of each experiment.

The number of counts in a coincidence spectrum peak was determined by a least-squares fit of a Gaussian peak and linear background to the experimental data points, by means of a computer program.

The distance between the source and the Si(Li)

detector was measured with a traveling microscope, and was found to be 20.5 mm. This source-to-detector distance was the same for all experiments involving conversion electrons. The diameter of the source itself was approximately 5.4 mm.

The geometrical corrections to the correlation coefficients were carried out by two methods. The first method was simply a correction for detector solid angle. The second method was a procedure developed by Feingold and Frankel [27] which incorporates a correction for source size together with the correction for detector solid angle. As explained in Appendix B, the two correction procedures gave practically identical results.

The coincidence resolving time of the system was measured by a method employing two radioactive sources well-separated from each other. The measurement yielded 2τ = 49 nanoseconds.

Correlations Involving Conversion Electrons

The three directional correlations measured involving conversion electrons were those of the $198\gamma/110e_L$, $198e_L/110\gamma$, and $177e_L/130.5\gamma$ cascades. In each case, the single-channel analyzer following the Si(Li) detector was adjusted to accept the conversion electron energy desired, and to exclude all other energies in so far as possible. The results of measurements on these cascades are summarized in Table 1.

Table 1. Summary of Experimental Results for Correlation Measurements Involving Conversion Electrons of Tm^{169}

R denotes the ratio of the real coincidence rate at 180° to the accidental coincidence rate. S is the ratio of the real coincidence rate at 90° to that at 270°. The estimated uncertainties in A_{22} and A_{44} are standard deviations.

Cascade	R	S	A_{22}	A_{44}
$198\gamma/110e_L$	3.5	1.02	-0.012±0.011	0.050±0.015
$198e_L/110\gamma$	20	0.995	0.106±0.012	-0.043±0.015
$177e_L/130.5\gamma$	21	1.015	-0.007±0.011	-0.051±0.015

198γ/110e_L Cascade

The electron analyzer "window" used is indicated by segment A of the ordinate axis of Figure 4. The distance from the source to the front face of the Ge(Li) crystal was 8.8 cm. The geometrical correction factors were: $Q_2(e)$ = 0.9357, $Q_4(e)$ = 0.7965, $Q_2(\gamma)$ = 0.978, $Q_4(\gamma)$ = 0.927. The values of $Q_2(e)$ and $Q_4(e)$ are the same throughout all these experiments. A total of about 10,000 real coincidence counts was accumulated at the 180° position.

198e_L/110γ Cascade

Segment B in Figure 4 indicates the electron analyzer window used. The distance from the source to the Ge(Li) detector was 8.1 cm. The Ge(Li) geometrical correction factors were: $Q_2(\gamma)$ = 0.974, $Q_4(\gamma)$ = 0.914. About 10,200 real coincidence counts were obtained at 180°.

177e_L/130.5γ Cascade

The electron analyzer setting is indicated by segment C in Figure 4. The Ge(Li) detector was 8.1 cm from the source. The correction factors for this detector were: $Q_2(\gamma)$ = 0.974, $Q_4(\gamma)$ = 0.914. A total of approximately 9290 real coincidence counts was collected at 180°.

Gamma-Gamma Directional Correlations

The two gamma-gamma directional correlations investigated were those of the 198γ/110γ and the 177γ/130.5γ

cascades. Two Ge(Li) detectors were used in these measurements. The results are summarized in Table 2.

For the 198γ/110γ cascade, the single-channel analyzer following the stationary ORTEC detector was adjusted to accept only the 198 keV gamma line. The source-to-detector distances for the stationary and moveable detectors were 7.5 cm and 8.1 cm, respectively. The geometrical correction factors were: $Q_2(198) = 0.972$, $Q_2(110) = 0.972$, $Q_4(198) = 0.908$, $Q_4(110) = 0.908$. The total number of real coincidence counts at 180° was about 43,700.

For the 177γ/130.5γ cascade, the analyzer was made to accept only the 177 keV gamma line. The stationary detector was at the same distance from the source as in the 198γ/110γ experiment, and the moveable detector was at a distance of 8.0 cm. The geometrical correction factors were: $Q_2(177) = 0.972$, $Q_2(130.5) = 0.972$, $Q_4(177) = 0.906$, $Q_4(130.5) = 0.908$. About 40,800 real coincidence counts were recorded at the 180° position.

Table 2. Summary of Experimental Results for Correlation Measurements on Gamma-Gamma Cascades in Tm^{169}

See Table 1 for definitions of symbols used.

Cascade	R	S	A_{22}	A_{44}
198γ/110γ	9.7	1.04	0.320±0.006	-0.018±0.007
177γ/130.5γ	14	0.98	0.257±0.007	0.015±0.009

CHAPTER IV

INTERPRETATION OF RESULTS, AND CONCLUSIONS

The gamma-gamma directional correlation coefficients of type A_{22} that are listed in Table 2 are compatible with the range of experimental values obtained by other investigators (15,18-25). The A_{44} coefficient for the 177γ/130.5γ correlation is within the range of previous measurements of this quantity, while A_{44} for the 198γ/110γ correlation is somewhat less than published values.

The values of $A_{22}(e_L,\gamma)/A_{22}(\gamma,\gamma)$, or $A_{22}(\gamma,e_L)/A_{22}(\gamma,\gamma)$, as the case may be, are listed in Table 3. Each such ratio, denoted by b_2^L, is a weighted sum of particle parameters for the L subshells. (For brevity, quantities such as b_2^L or b_4^L will hereafter be referred to as particle parameters, also.) Also tabulated are the theoretical values for these same quantities. The latter were calculated on the basis of theoretically computed particle parameters (7) and partial internal conversion coefficients (8) and the experimentally determined mixing ratio (17) for the transition in question.

Experimentally Determined Particle Parameters

When the electron-gamma correlation experiments were first undertaken, the gamma rays were used for the coincidence gates. However, the congested nature of the conversion

Table 3. Theoretical and Experimental Particle Parameters, of Type b_2, for Transitions in Tm^{169}

Theoretical values are listed for the L_1, L_2, and L_3 subshells, and for the total L and M shells, together with the experimental results obtained in this investigation for the total L shell.

Shell, or Subshell	b_2(198 keV)	b_2(177 keV)	b_2(110 keV)
L_1	0.1675	0.0846	0.0388
L_2	1.2475	0.2226	1.0042
L_3	1.2977	-0.0686	0.8908
L (total)	0.358	0.093	0.179
M (total)	0.368	0.101	0.198
L, Expt.	0.331±0.038	-0.027±0.045	-0.037±0.036

electron spectrum (or alternatively, the lack of resolution of the Si(Li) detector), together with a not inconsiderable accidental coincidence rate in some cases, made the process of separating the peaks (in the coincidence spectra) and the determination of the areas of the peaks very difficult and sensitive to small perturbations of the analysis procedure. Therefore, the decision was made to gate on the conversion electrons instead, although this procedure would not give as pure a gate as the other method did.

b_2^L(198 keV)

The experimental value of b_2^L(198 keV) is 0.331±0.038, and the theoretically calculated value is 0.358. Thus, the experimental and theoretical values are essentially in agreement.

b_2^L(177 keV)

For the 177 keV transition, the value b_2^L = -0.027±0.045 was obtained. The theoretical value is 0.093. This discrepancy is somewhat unexpected in view of the basic agreement for the 198 keV transition. However, the halflife of the 139 keV level (the intermediate state for the 177 keV/130.5 keV cascade) is about four times as long as the halflife of the 118 keV level (the intermediate state for the 198 keV/110 keV cascade). Moreover, the magnetic dipole moment for the 139 keV level is greater than the magnetic moment of the 118 keV level by a factor of roughly

1.8. Thus, $(\mu\tau)_{139} \simeq 8\times(\mu\tau)_{118}$. It may be possible that a hyperfine interaction between the Tm^{169} nucleus at the 139 keV level and the disrupted electron shell (following the first transition, which was converted) is sufficient to considerably affect the $177e_L/130.5\gamma$ correlation, whereas the same type of interaction might not be able to affect the $198e_L/110\gamma$ correlation to nearly the same extent.

b_2^L(110 keV)

For the 110 keV transition, the b_2^L value found was -0.037 ± 0.036. The theoretically predicted value is 0.179. The cascade used in the measurement of b_2(110 keV) was the same one as used in the measurement of b_2(198 keV), and furthermore the first transition was not converted in this case. Presumably then, a hyperfine interaction between the nucleus and the electron shell would not be responsible for the difference between the experimental and theoretical values. The kinetic energy of the converted L shell electrons for this transition is about 100 keV, which is a relatively low energy. So in this case, it may be that electron scattering in the source had a significant effect on the correlation.

b_4^L Values for the 198 keV, 177 keV, and 110 keV Transitions

The experimental values for the quantities b_4^L (in Table 4) are probably inconclusive, because of the relatively large uncertainties in the $A_{44}(\gamma,\gamma)$ correlation coefficients.

Table 4. Theoretical and Experimental Particle Parameters, of Type b_4, for Transitions in Tm^{169}

The format follows that of Table 3.

Shell, or Subshell	b_4(198 keV)	b_4(177 keV)	b_4(110 keV)
L_1	-0.1604	-0.1800	-0.1542
L_2	2.8498	2.3391	6.6515
L_3	4.5342	2.9412	13.7091
L (total)	0.450	0.509	1.154
M (total)	0.524	0.588	1.287
L, Expt.	$2.39^{+2.9}_{-1.3}$	$-3.40^{+1.9}_{-7.6}$	$-2.78^{+1.4}_{-3.1}$

CHAPTER V

SUGGESTIONS FOR FUTURE RESEARCH

The relatively crowded nature of the Tm^{169} conversion electron spectrum seems to demand a degree of resolution such as would only be available in a deflection type spectrometer. A system employing a magnetic spectrometer for selection of conversion electrons and a sodium iodide gamma detector would probably be adequate for study of several of the directional correlations available in Tm^{169}. Some cascades other than the ones considered in this investigation are those of 198 keV/110 keV and 177 keV/110 keV.

APPENDICES

APPENDIX A

OUTLINE OF THE THEORETICAL FORMALISM

For an investigation such as this, the fundamental results of directional correlation theory are contained in equations (I-1), (I-2), and (I-3), together with the definitions of the quantities appearing in those equations. The development of the theory is presented in this appendix in outline form, primarily as a summary of the detailed treatment by H. J. Rose and D. M. Brink (5). Other expositions of the general theory of angular correlations are those of L. C. Biedenharn and M. E. Rose (3,28), Biedenharn (4), and Frauenfelder and Steffen (1).

Transition Probability for Emission of Gamma Rays

The basic problem is to derive an expression for the transition probability, ω, from an initial nuclear state $|\lambda>$ to a final state consisting of the nuclear state $|\mu>$ and a photon state $|\vec{k},\vec{\varepsilon}>$. Here, $\vec{k}$ is the propagation vector of the photon and $\vec{\varepsilon}$ is the photon polarization vector. We set $k = |\vec{k}|$, and take $|\vec{\varepsilon}| = 1$. From first-order perturbation theory, we have

$$\omega(\lambda \rightarrow \mu + (\vec{k},\vec{\varepsilon})) = \frac{2\pi}{\hbar} \; |<\mu,(\vec{k},\vec{\varepsilon})|V|\lambda>|^2 \; \rho(E), \qquad \text{(A-1)}$$

where V is the interaction producing the transition, and $\rho(E)$ is the density of final continuum photon states. The photon energy, E, is equal to $\hbar ck$.

Next, we use the standard technique of normalizing the photon states in a cubical box with side L, and periodic boundary conditions. For photons with a definite polarization, the density of states per unit energy per unit solid angle is

$$\rho(E) = \frac{L^3 k^2}{\hbar c (2\pi)^3} . \qquad \text{(A-2)}$$

From quantum field theory, the interaction V can be expressed as

$$V = -\left(\frac{e\hbar}{2mc}\right) \sum_n \left(2g_{\ell n}\vec{p}_n\cdot\vec{A}(\vec{r}_n) + g_{sn}\vec{S}_n\cdot\vec{H}(\vec{r}_n)\right). \qquad \text{(A-3)}$$

The quantities $g_{\ell n}$ and g_{sn} are orbital and spin g-factors, respectively, for the n'th nucleon. The vector potential $\vec{A}$, appearing in the preceding equation is a field operator and may be expanded in the form

$$\vec{A}(\vec{r}) = \sum_{k,\eta} \left(\frac{2\pi\hbar c}{L^3 k}\right)^{\frac{1}{2}} [\vec{\varepsilon}_\eta \exp(i\vec{k}\cdot\vec{r}) a_{k\eta} + \vec{\varepsilon}^*_\eta \exp(-i\vec{k}\cdot\vec{r}) a^+_{k\eta}]. \qquad \text{(A-4)}$$

In Eq. (A-3), $\vec{H}(\vec{r}_n) = \text{curl}(\vec{A}(\vec{r}_n))$. The quantities $a^+_{k\eta}$ and $a_{k\eta}$ are creation and annihilation operators, respectively,

for a photon with wave vector $\vec{k}$ and polarization $\vec{\varepsilon}_\eta$. (The superscript "+" denotes the operator adjoint, and "*" denotes the complex conjugate.)

On substituting Eq. (A-4) into Eq. (A-3), V may be expressed in the form

$$V = \sum_{k,\eta} \left(\frac{2\pi\hbar c}{L^3 k}\right)^{\frac{1}{2}} [H_a(\vec{k},\vec{\varepsilon}_\eta) a_{k\eta} + H_e(\vec{k},\vec{\varepsilon}_\eta) a^+_{k\eta}], \tag{A-5}$$

where,

$$H_a(\vec{k},\vec{\varepsilon}) = -\left(\frac{e\hbar}{2mc}\right)[2\, g_\ell \vec{p}\cdot\vec{\varepsilon}\, \exp(i\vec{k}\cdot\vec{r}) + g_s\, \vec{S}\cdot \mathrm{curl}\{\vec{\varepsilon}\, \exp(i\vec{k}\cdot\vec{r})\}], \tag{A-6}$$

and

$$H_e(\vec{k},\vec{\varepsilon}) = [H_a(\vec{k},\vec{\varepsilon})]^+. \tag{A-7}$$

In the last three equations, and from here on, it is implicitly assumed that the sum over all individual nucleons has been carried out.

Noting that only the term in V which contains the creation operator for the photon state $(\vec{k},\vec{\varepsilon}_\eta)$ will contribute to the matrix element of Eq. (A-1), we have

$$\langle \mu, (\vec{k},\vec{\varepsilon}) | V | \lambda \rangle = \left(\frac{2\pi\hbar c}{L^3 k}\right)^{\frac{1}{2}} \langle \lambda | H_a(\vec{k},\vec{\varepsilon}) | \mu \rangle^* , \tag{A-8}$$

whence

$$\omega(\lambda \to \mu + (\vec{k},\vec{\varepsilon})) = \frac{k}{2\pi\hbar} \left| \langle \lambda | H_a(\vec{k},\vec{\varepsilon}) | \mu \rangle \right|^2 . \qquad \text{(A-9)}$$

The next step is to express the matrix element appearing in Eq. (A-9) in terms of matrix elements of certain interaction multipole operators, $T^{(\pi)}_{LM}$. Following a series of straightforward, but somewhat lengthy, manipulations the Hamiltonian $H_a(\vec{k},\vec{\varepsilon}_q)$ (for a circularly polarized plane wave interacting with nucleons) can be written as

$$H_a(\vec{k},\vec{\varepsilon}_q) = - \sum_{L,M,\pi} q^{\pi} \, T^{(\pi)}_{LM} \, D_{Mq}{}^{L}(R). \qquad \text{(A-10)}$$

The multipole operators $T^{(\pi)}_{LM}$ transform like spherical tensors of rank L under rotations. The superscript π takes the value zero for electric interaction multipole operators, and unity for magnetic multipole operators. The circular polarization is denoted by q, and q can only be 1 or -1. The D^{L}_{Mq} are rotation matrices. R is the rotation which takes the z-axis into the direction $\vec{k}$.

For a nuclear state which is aligned with respect to an axis of cylindrical symmetry, the states $|\lambda\rangle$ and $|\mu\rangle$ can be specified in terms of their angular momentum quantum numbers, $|\lambda\rangle = |J_1 M_1\rangle$ and $|\mu\rangle = |J_2 M_2\rangle$. The magnetic quantum numbers M_i refer to the axis of cylindrical symmetry.

Next, we assume that the orientation of the spin J_2 is not observed. Then the probability, $P_{M_1}^{q}(\vec{k})$, for emission from the initial state is given by

$$P_{M_1}^{q}(\vec{k}) = \sum_{M_2} \omega(J_1 M_1 \rightarrow J_2 M_2 + (\vec{k}, \vec{\varepsilon}_q)). \qquad \text{(A-11)}$$

Making use of Eqs. (A-9) and (A-10), we may write

$$P_{M_1}^{q}(\vec{k}) = \left(\frac{k}{2\pi\hbar}\right) \sum_{M_2} \left| \sum_{L,M,\pi} {}^{q}\pi \langle J_1 M_1 | T_{LM}^{(\pi)} | J_2 M_2 \rangle D_{Mq}^{L}(R) \right|^2. \qquad \text{(A-12)}$$

If the polarization is not observed, then an incoherent sum over q must be performed.

We now restrict attention to the case that the radiating system is in a cylindrically symmetric environment. With the z-axis chosen to be along the symmetry axis, M_1 is a constant of the motion. Hence, the total radiative probability, $P^{q}(\vec{k})$, for photons along $\vec{k}$ will be found by weighting each $P_{M_1}^{q}(\vec{k})$ with the population probability $\nu(M_1)$ of the substate M_1, and summing.

$$P^{q}(\vec{k}) = \sum_{M_1} \nu(M_1)\, P_{M_1}^{q}(\vec{k}). \qquad \text{(A-13)}$$

Here, $\sum_{M_1} \nu(M_1) = 1$, and $P_{M_1}^{q}(\vec{k})$ is given by Eq. (A-12).

Making use of the Wigner-Eckart theorem,

$$\langle J_1 M_1 | T_{LM} | J_2 M_2 \rangle = (-1)^{2L} (J_2, L, M_2, M | J_1, M_1) \times \langle J_1 || T_L || J_2 \rangle, \tag{A-14}$$

and the properties of the rotation matrices D_{Mq}^{L}, and after considerable algebraic manipulation, we find that the total radiative probability, $P(\vec{k})$, after summing over unobserved circular polarization states, is given as

$$P(\vec{k}) = \left(\frac{k}{2\pi\hbar}\right) \sum_{L,L',K,\pi,\pi'} B_K(J_1)\, R_K(L,L',J_1,J_2)\, P_K(\cos(\theta)) \times$$

$$\left[1+(-1)^{L+L'+\pi+\pi'-K}\right] \frac{\langle J_1 || T_L^{(\pi)} || J_2 \rangle}{(2L_1+1)^{1/2}} \times \frac{\langle J_1 || T_{L'}^{(\pi')} || J_2 \rangle^*}{(2L'+1)^{1/2}} . \tag{A-15}$$

The quantities appearing in Eq. (A-15) which have not been previously defined are given below:

$$B_K(J_1) = \sum_{M_1} \left[\nu(M_1)(-1)^{J_1-M_1}(2J_1+1)^{\frac{1}{2}} \times (J_1, J_1, M_1, -M_1 | K, 0)\right]; \tag{A-16}$$

$$R_K(L,L',J_1,J_2) = (-1)^{1+J_1-J_2+L'-L-K} \times$$

$$\left[(2J_1+1)(2L+1)(2L'+1)\right]^{\frac{1}{2}} (L,L',1,-1|K,0) \times W(J_1,J_1,L,L';K,J_2). \tag{A-17}$$

$W(J_1,J_1,L,L':K,J_2)$ is a Racah coefficient.

The mixing ratio is defined as

$$\delta_L^{(\pi)} = \frac{\langle J_1||T_L^{(\pi)}||J_2\rangle/(2L+1)^{1/2}}{\langle J_1||T_L^{(\pi)}||J_2\rangle/(2L+1)^{1/2}} . \qquad \text{(A-18)}$$

It can always be chosen to be real, which we assume has been done. The lowest-order multipolarity occurring in the transition is denoted by L,π. We will now express Eq. (A-15) in terms of mixing ratios, for the case that the initial and final states have definite parity. Since the electromagnetic interaction conserves parity, the sum $(L+L'+\pi+\pi')$ must be an even integer. Hence, only even values of K will appear. The quantity P(k) will be replaced by $W(\theta)$, to which it is proportional, where the normalization is chosen such that the coefficient of $P_0(\cos(\theta))$ in the expansion of $W(\theta)$ is unity.

$$W(\theta) = \sum_{\substack{(L\pi)(L'\pi') \\ k \text{ even}}} \frac{B_K(J_1)R_K(L,L',J_1,J_2)\delta_L^{(\pi)}\delta_{L'}^{(\pi')}P_K(\cos(\theta))}{\Sigma_L(\delta_L^{(\pi)})^2} \qquad \text{(A-19)}$$

The sum over $(L\pi)$ is over all multipoles consistent with the conservation of angular momentum and parity. L and L' are allowed to have values between $|J_1-J_2|$ and (J_1+J_2), inclusive, with neither L nor L' equal to zero. In Eq. (A-19),

the factor $B_K(J_1)$ depends only on the nuclear alignment, while the factor

$$\sum_{(L\pi)(L'\pi')} \frac{R_K(L,L',J_1,J_2)\delta_L^{(\pi)}\delta_{L'}^{(\pi')}}{\Sigma_L\,(\delta_L^{(\pi)})^2}$$

depends only on quantities characterizing the nuclear transition. Eq. (A-19) gives the angular distribution in terms of mixing ratios for a gamma ray originating from the decay of state J_1, with the alignment of the state specified by $B_K(J_1)$.

Case of Angular Correlation

For the case of angular correlations, the initial state J_1 is randomly populated and subsequently decays by emission of a sequence of at least two gamma rays. We shall consider only the simplest case that the two gamma rays observed in coincidence are the first and second ones of the cascade originating from the decay of J_1. The alignment is attained by observation of the first gamma ray. Since the state J_1 is randomly populated there is no preferred direction in space, and we choose the axis of quantization (z-axis) to be the direction of propagation of the first gamma ray. The magnetic substates M_1 are specified with respect to this axis, and the wavefunctions $|J_1M_1\rangle$ are chosen so as to be eigenstates of $\hat{J}_{1z}$. The population weighting of the first state is

given by $\nu(M_1) = (2J_1+1)^{-1}$.

Now the circular polarization q of the first gamma ray is specified with respect to the z-axis, so the relation $M_2+q = M_1$ follows. Hence, M_2 will be "sharp" with respect to the z-axis; or in other words, there are wavefunctions $|J_2M_2\rangle$ such that M_2 is an eigenvalue of $\vec{J}_{2z}$. In our case, only the second gamma ray of the cascade is detected (at an angle θ relative to the first ray), so the z-axis is an axis of cylindrical symmetry. Thus, the directional distribution of the second observed gamma ray ($J_2 \rightarrow J_3$) can also be described by Eq. (A-15) after replacement of J_1 by J_2, and J_2 by J_3. All that remains is to calculate the populations $\nu(M_2)$.

To this end, we recall that for a given value of q there is only one M_2 corresponding to each M_1. Then the probability, $W^{q_1}(M_2)$, of populating M_2 from M_1 will be given by weighting each $\omega(J_1M_1 \rightarrow J_2M_2+(\vec{k}_1,\vec{\varepsilon}_{q_1}))$ with the statistical weight of M_1, which is $(2J_1+1)^{-1}$, and summing over M_1. That is,

$$W^{q_1}(M_2) = (2J_1+1)^{-1} \sum_{M_1} \omega(J_1M_1 \rightarrow J_2M_2+(\vec{k}_1,\vec{\varepsilon}_{q_1})). \qquad \text{(A-20)}$$

Each $\omega(J_1M_1 \rightarrow J_2M_2+(\vec{k}_1,\vec{\varepsilon}_{q_1}))$ can be expressed in terms of the interaction multipole operators by substituting Eq. (A-10) into Eq. (A-9). When this has been done, and after considerable

algebraic manipulation, $W^{q_1}(M_2)$ can be written in terms of $B_K{}^{q_1}(J_2)$. Quantities of the latter type are summed over q_1 to give $B_K(J_2)$, with the result that, if K is an even integer,

$$B_K(J_2) = \sum_{(L_1\pi_1)(L_1'\pi_1')} [(-1)^{L_1-L_1'} R_K(L_1,L_1',J_2,J_1) \delta_{L_1}^{(\pi_1)} \delta_{L_1'}^{(\pi_1')}] \times$$

$$2 \sum_{N_1} (\delta_{N_1}^{(\pi_1)})^2]^{-1}. \qquad \text{(A-21)}$$

If K is odd, the $B_K(J_2) = 0$. Eq. (A-21) assumes that all nuclear states have definite parity.

For the usual case that only two multipolarities need be considered, then Eq. (A-21) reduces to

$$B_K(J_2) = [R_K(L_1,L_1,J_2,J_1) + (-1)^{\bar{L}_1-L_1} 2\delta_1 \times$$

$$R_K(L_1,\bar{L}_1,J_2,J_1) + \delta_1{}^2 R_K(\bar{L}_1,\bar{L}_1,J_2,J_1)] \times (1+\delta_1{}^2)^{-1}, \qquad \text{(A-22)}$$

for even K. Here, L_1 and $\bar{L}_1$ are the two lowest possible multipolarities, with $\bar{L}_1 = L_1 + 1$.

We can now obtain the final expression for the directional correlation function, W, by inserting $B_K(J_2)$, as given in Eq. (A-21), into Eq. (A-19). For the case that both the populating transition and the following transition are

contributed to by two multipolarities, the result is

$$W(\theta) = \sum_{K \text{ even}} [R_K(L_1,L_1,J_2,J_1) - 2\delta_1 R_K(L_1,\bar{L}_1,J_2,J_1) +$$

$$\delta_1^2 R_K(\bar{L}_1,\bar{L}_1,J_2,J_1)](1+\delta_1^2)^{-1} \times$$

$$[R_K(L_2,L_2,J_2,J_3) + 2\delta_2 R_K(L_2,\bar{L}_2,J_2,J_3) +$$

$$R_K(\bar{L}_2,\bar{L}_2,J_2,J_3)](1+\delta_2^2)^{-1} P_K(\cos(\theta)). \qquad \text{(A-23)}$$

Here, $\bar{L}_1 = L_1+1$ and $\bar{L}_2 = L_2+1$.

The highest possible value of K is determined by certain "triangular" conditions governing Clebsch-Gordon and Racah coefficients contained in the B_K's and in the R_K's. The result is $K \leq \min(2J_2, 2\bar{L}_1, 2\bar{L}_2)$. The coefficients of type R_K which appear in Eq. (A-23) are related to the F_K coefficients mentioned in Chapter I in the following manner:

$$R_K(L,L',J_1,J_2) = (-1)^{L-L'+K} F_K(L,L',J_2,J_1). \qquad \text{(A-24)}$$

From Eq. (A-23) it can be seen that the coefficient multiplying $P_K(\cos(\theta))$ is a product of two terms each of which depends on only one transition of the cascade. Denoting the coefficient of P_K by A_{KK}, we can write

$$A_{KK} = A_K(J_1 \to J_2)\ A_K(J_2 \to J_3). \qquad \text{(A-25)}$$

Directional Correlation Particle Parameters for Conversion Electrons

For directional correlations between electrons and gamma rays, the correlation function W is modified in that each R_K coefficient (or F_K coefficient, see Eq. (A-24)) for the converted transition is multiplied by an electron particle parameter, b_K (3). If the converted transition is of mixed multipolarity, then the gamma mixing ratio (δ) for that transition is replaced by the quantity $\delta(\alpha_{\tilde{L}}/\alpha_L)^{1/2}$, where the α's are the conversion coefficients for the two contributing multipolarities.

Formulas for the particle parameters may be found in references (3), (28), (29), and (30). Each particle parameter will depend on the multipolarity, parity, and energy of the transition, the atomic number (Z) of the nucleus, and the initial electron state (e.g., K-shell, L_2-subshell, etc.).

As an example, the particle parameters for magnetic 2^L-pole conversion of an L_1-subshell electron are given by,

$$b_K(ML) = 1 + \frac{K(K+1)}{2L(L+1)-K(K+1)} \frac{L(L+1)}{2L+1} \times \frac{|1-T_M(L)|^2}{L+1+L|T_M(L)|^2} ; \qquad (A\text{-}26)$$

$$\text{where } T_M(L) = \frac{[\exp(i\eta_\nu)R^M_{\nu,\nu'}]_{\nu'=-1,\nu=L+1}}{[\exp(i\eta_\nu)R^M_{\nu,\nu'}]_{\nu'=-1,\nu=-L}} . \qquad (A\text{-}27)$$

$$\text{Here, } R^{M}_{v,v'} = \int_{o}^{\infty} h_L(f_v g_{v'} + f_{v'} g_v) r^2 dr, \qquad \text{(A-28)}$$

η_v is a phase factor, and h_L is the spherical Hankel function of order L. The functions f and g are radial wave-functions satisfying the Dirac equations. The quantum numbers v' and v refer to the bound and continuum electron states, respectively.

The theoretical particle parameters used in this investigation were interpolated from particle parameter values calculated by Hager and Seltzer (7).

APPENDIX B

ANALYSIS OF EXPERIMENTAL DATA

As mentioned previously, coincidence counts were stored in the computer core during the actual data collection time at a given angle. At the end of a counting period, the computer program normalized the number of counts in core for each energy channel to the length of that counting interval and to the singles counting rate in the moveable detector for that same interval. The normalization to the singles counting rate makes a first-order correction for source de-centering, and makes the measured correlation function independent of the source decay (1, p. 1191). The normalized counting rates were averaged in with any previous counting rate data at the given angle, and stored on a magnetic disk. The counting rate data for accidental coincidences was taken separately from the real-plus-accidental coincidence data. The accidental rates from all counting positions were averaged together and stored as one rate.

At the conclusion of an experiment on a cascade, it was necessary to determine the true coincidence counting rate at each angle. This was accomplished in the manner now outlined.

A function consisting of one (or more) Gaussian

peak(s) and a linear background was least-squares-fitted to each coincidence spectrum stored by the computer. The coincidence counting rate obtained for the appropriate gamma radiation would be represented by the area of one of the fitted Gaussian peaks. The real coincidence rate at an angle was obtained by subtracting the accidental rate from the real-plus-accidental rate at that angle.

For a one-peak spectrum, the function to be fitted to the data could be written as

$$F(x,\vec{c}) = c_1 - c_2 x + c_3 \exp\left[-\frac{1}{2}\left(\frac{x-c_4}{c_5}\right)^2\right]; \qquad \text{(B-1)}$$

where x represents the channel number of the energy spectrum, the vector $\vec{c} = (c_1, c_2, c_3, c_4, c_5)$, and the c_n's (n=1,...,5) are real numbers yet to be determined. As defined in Eq. (B-1), F is a nonlinear function of the c_n's.

The least-squares criterion specifies that $\vec{c}$ should be chosen such that the function G, defined in the following equation, is minimized.

$$G(\vec{c}) = \sum_i \left(\frac{y_i - F(x_i,\vec{c})}{\sigma_i}\right)^2 , \qquad \text{(B-2)}$$

where y_i is the coincidence counting rate in the i'th channel, and σ_i is the standard deviation in y_i which is appropriate for a Poisson distribution of counts in channel x_i.

The computer program which performed the task of minimizing G had been adapted earlier from one given by Bevington (31). The point $(\bar{c}_1,\bar{c}_2,\bar{c}_3,\bar{c}_4,\bar{c}_5)$ in parameter space at which G takes its minimum value gives the "best" values (in this context) for the coefficients, c_n, in Eq. (B-1). The area of the fitted peak can then be found from the coefficients $\bar{c}_3$ and $\bar{c}_5$.

The extension of this spectrum-fitting procedure to a multipeak spectrum is straightforward, in principle. However, difficulties of a practical nature can arise, particularly if a ridge is formed by several peaks fairly close together.

After finding the real coincidence counting rate at each angle, it is then necessary to least-squares-fit to these data an experimental correlation function, w, of the form

$$w(\theta) = a_0 + a_2P_2(\cos(\theta)) + a_4P_4(\cos(\theta)). \qquad \text{(B-3)}$$

As in the previous case with the c_n's, the coefficients a_0, a_2, and a_4 are to be considered as adjustable parameters. Denoting the real coincidence counting rate at the angle θ by $R(\theta)$, the function U was defined in the manner,

$$U(a_0,a_2,a_4) = \sum_i \left(\frac{R(\theta_i)-w(\theta_i)}{\sigma_i}\right)^2 . \qquad \text{(B-4)}$$

The sum over the index i means a sum over the angles (θ_i) at which coincidence data were taken. Those angles were 90°, 135°, 180°, 225°, and 270°. Here σ_i is the standard deviation in $R(\theta_i)$. Since w, of Eq. (B-3), is linear in the a's, the minimization of U is far simpler than the corresponding problem with G.

If U takes its minimum at $(\bar{a}_0,\bar{a}_2,\bar{a}_4)$, then the correlation coefficients A'_{22} and A'_{44} are defined as $A'_{22} = \bar{a}_2/\bar{a}_0$, and $A'_{44} = \bar{a}_4/\bar{a}_0$. Lastly, A'_{22} and A'_{44} must be corrected for effects arising from the solid angles subtended by the detectors and the size of the source.

Tables 5, 6, and 7 present samples of the data and results of the least-squares fitting procedures for one of the experiments conducted.

At each stage of the data analysis process, the estimation and/or propagation of the random errors was carried out according to standard statistical procedures (31).

Corrections for Detector Solid Angles and Source Size

M. E. Rose (32) has worked out the procedure to be followed in making solid angle corrections for the case of a point source at the intersection of the axes of two cylindrically symmetric detectors (assuming no counter-to-counter scattering of radiations). For this case, it turns out that the corrected coefficient A_{kk} is given as

Table 5. Normalized Coincidence Rates for the $198e_L/110\gamma$ Cascade in Tm^{169}

Channel No.	90°	135°	180°	225°	270°	Acc.
1	2595	2523	2532	1889	2969	1030
2	2408	2248	2755	3101	2549	687
3	2529	2113	2559	2600	3019	562
4	2738	3092	2300	3087	2663	744
5	3000	2644	2785	3366	2642	819
6	3031	2359	2682	2300	2483	607
7	2835	2382	2632	2550	2862	762
8	2938	2530	1989	2558	3244	631
9	2677	2332	3020	2819	3222	829
10	2776	2577	3101	2569	2315	682
11	2760	2809	3130	2664	3131	918
12	3511	2830	4000	3798	3137	2241
13	4075	2689	3545	3157	3692	1383
14	2662	3076	2871	2862	2762	1808
15	2870	2605	2531	2346	2751	1222
16	2886	2613	2506	2476	2315	509
17	2072	2790	2760	2631	2981	693
18	2720	2945	2814	2678	2198	324
19	2840	2983	3046	3246	2642	435
20	3131	3115	3682	2846	3350	567
21	4004	3914	4376	3996	3461	1120
22	5400	6093	6528	6447	5493	1170
23	16467	15797	15705	19662	16085	999
24	47476	49249	49341	51847	45638	1829
25	87393	92988	99991	90614	89103	7720
26	55542	59941	64325	55894	59698	3224
27	18181	20144	22238	18956	18440	2085
28	4913	6088	7107	5585	5578	1416
29	3277	3450	3892	3157	3686	854
30	5361	4944	5140	5057	4616	630
31	8996	8234	8698	9483	10236	990
32	10214	9734	9609	9398	10972	1163
33	5494	5291	5160	5197	5100	713
34	1677	2660	2204	2199	2376	741
35	1168	1010	1194	1561	1455	701

Table 5 (concluded)

Channel No.	90°	135°	180°	225°	270°	Acc.
36	1795	1186	1095	960	893	651
37	1150	1337	1318	1333	1145	375
38	630	1312	1335	1105	1029	498
39	1634	1414	2033	1752	1346	848
40	3020	3038	3283	3621	3418	1506
41	4877	5003	5534	5129	5205	2299
42	4269	5108	3733	4061	4119	2606
43	2165	2150	2090	2265	1953	1543
44	660	957	1287	956	745	799
45	380	652	1155	505	542	1007
46	573	474	829	708	227	571
47	703	384	704	519	373	425
48	360	645	463	356	309	341
49	346	613	568	390	503	135

Table 6. Some Results of Statistical Analysis of the Data for the $198e_L/110\gamma$ Cascade in Tm^{169}

Parameters resulting from a least-squares fit of three Gaussian peaks and a linear background to the data of Table 5. Numerical entries have been rounded to four digits. For $n \geq 6$, c_n is analogous to c_{n-3}. See Eq. (B-1).

	90°	135°	180°	225°	270°	Acc.*
c_1	36.86	32.05	31.99	34.62	36.51	95.16
c_2	.5846	.4485	.4091	.5228	.5838	.4907
c_3	850.7	853.6	851.8	843.5	858.4	800.6
c_4	25.08	25.10	25.13	25.03	25.12	25.11
c_5	1.033	1.028	1.004	1.065	1.021	.6398
c_6	88.68	74.64	68.53	82.29	98.34	63.95
c_7	31.55	31.60	31.52	31.50	31.56	31.68
c_8	1.126	1.183	1.143	1.130	1.034	.5237
c_9	39.71	40.78	34.25	38.47	41.55	226.9
c_{10}	41.31	41.43	41.11	41.16	41.19	41.63
c_{11}	.9930	.9318	.8347	1.049	.9615	1.181

*The "Acc." rates were fitted with four Gaussian peaks. The parameters for the remaining peak are not shown.

The parameters c_3, c_4, and c_5 correspond to the 110 keV gamma coincidence peak.

Table 7. Further Results of Analysis of Data for the $198e_L/110\gamma$ Cascade in Tm^{169}

In this table, C_T denotes the total number of counts in the 110 keV gamma coincidence peak, and R denotes the normalized counting rate (counts per 100 sec.) for this peak.

	90°	135°	180°	225°	270°	Acc.
C_T	4791	5130	10694	5161	4788	176.2
R	2.832	3.032	3.193	3.186	2.845	0.1497

- -

The parameters resulting from a least-squares fit of an experimental correlation function (Eq. (B-3)) to the preceding counting rates are listed below, together with the uncorrected coefficients A'_{22} and A'_{44}.

a_0	a_1	a_2	A'_{22}	A'_{44}
2.855	0.2738	-0.0891	0.096	-0.031

$$A_{kk} = \frac{A'_{kk}}{Q_k(D_1)Q_k(D_2)} , \qquad (B\text{-}5)$$

for each value of the index k. The total correction is seen to be split into two parts, each part depending on only one of the detectors. The correction factors take the form $Q_k = J_k/J_0$, where

$$J_k = \int_0^{\beta_{max}} P_k(\cos(\beta))\varepsilon(E,\beta)\sin(\beta)d\beta. \qquad (B\text{-}6)$$

Here, $\varepsilon(E,\beta)$ is the absorption efficiency of the detector for the type of radiation received, of energy E and at entrance angle β.

Camp and Van Lehn (33,34) have evaluated such integrals by numerical methods for several common sizes of cylindrically symmetric Gi(Li) detectors, and a range of gamma ray energies and source-to-detector distances. Their results were appropriate to the ORTEC detector. They also evaluated such integrals for the so-called "five-sided" trapezoidal Ge(Li) detectors. The Nuclear Diodes detector used in the experiments was of this latter type. Although not cylindrically symmetric, it was used with the assumption that its departure from this ideal shape was not severe enough to be a determining factor in the accuracy of results obtained. The computations of Camp and Van Lehn have been used to find, by interpolation, the Q_2 and Q_4 values for both the Ge(Li)

detectors used in this investigation.

As for the Si(Li) detector, the efficiency ϵ can be taken to be independent of β, the electron entrance angle. For this case, the integral of Eq. (B-4) can be evaluated analytically. Setting $\omega = \sin^2(\beta_{max}/2)$, the results for Q_2 and Q_4 are:

$$Q_2 = 1-3\omega+2\omega^2,$$

$$Q_4 = 1-10\omega+30\omega^2-35\omega^3+14\omega^4. \qquad \text{(B-7)}$$

If the radius of the circular electron detector is denoted by r_e and the distance from the source to the detector by R_e, then

$$\omega = \frac{1}{2}\left(1-\left[1+(r_e/R_e)^2\right]^{-\frac{1}{2}}\right). \qquad \text{(B-8)}$$

If the source is not a geometrical point, or if it is not centered, or if the detectors are not cylindrically symmetric, then the corrected coefficient A_{kk} may not be given by such a simple expression as in Eq. (B-5). In general, each A_{kk} would depend on all the coefficients of type $A'_{\ell\ell}$, and the index ℓ would range over odd as well as even integers.

Feingold and Frankel (27) have investigated the form taken by the measured correlation function for a small,

centered line source perpendicular to the plane containing the detector axes. Their results can be applied directly to the case of a small, centered disk source whose plane is parallel to the face of one of the (cylindrically symmetric) detectors, if the other detector is far enough away from the source to "see" it as a point. In the experiments previously described, the diameter of the (disk) source was about 5.4 mm, the distance from the source to the Si(Li) detector was about 20.5 mm, and the distance between the source and the Ge(Li) detector was roughly 80 mm. As a first approximation to correcting the measured correlation coefficients for source size, the results of Feingold and Frankel for the case cited were applied. The source size was assumed to be negligible as far as the Ge(Li) detector was concerned. For each experiment, the corrected coefficients obtained by this method were practically identical with those found using the simpler correction procedure. In each case, the difference in values for the coefficient corrected by the two methods was insignificant compared to the estimated standard deviation in that coefficient. Since the greater part of any source size correction should have been accounted for by using the procedure mentioned, it would seem that the aggregate effect of the source size was negligible.

BIBLIOGRAPHY

1. H. Frauenfelder and R. M. Steffen, Angular Correlations, in Alpha-, Beta-, and Gamma-Ray Spectroscopy (ed. K. Siegbahn), North-Holland Publishing Co., Amsterdam (1965) p. 997.

2. D. R. Hamilton, Phys. Rev. 58, 122 (1940).

3. L. C. Biedenharn and M. E. Rose, Rev. Mod. Phys. 25, 729 (1953).

4. L. C. Biedenharn, Angular Correlations in Nuclear Spectroscopy, in Nuclear Spectroscopy, Part B (ed. F. Ajzenberg-Selove), Academic Press, New York, (1960) p. 732.

5. H. J. Rose and D. M. Brink, Rev. Mod. Phys. 39, 306 (1967).

6. E. L. Brady and M. Deutsch, Phys. Rev. 72, 870 (1947).

7. R. S. Hager and E. C. Seltzer, Nuclear Data A4, 397 (1968).

8. R. S. Hager and E. C. Seltzer, Nuclear Data A4, 1 (1968).

9. S. A. E. Johansson, Phys. Rev. 100, 835 (1955).

10. J. M. Cork, M. K. Brice, D. W. Martin, L. C. Schmid, and R. G. Helmer, Phys. Rev. 101, 1042 (1956).

11. J. W. Mihelich, T. J. Ward, and K. P. Jacob, Phys. Rev. 103, 1285 (1956).

12. E. N. Hatch, F. Boehm, P. Marmier, and J. W. M. DuMond, Phys. Rev. 104, 745 (1956).

13. B. R. Mottelson and S. G. Nilsson, Mat. Fys. Skr. Dan. Vid. Selsk. 1, No. 8 (1959).

14. A. E. Blaugrund, Y. Dar, and G. Goldring, Phys. Rev. 120, 1328 (1960).

15. C. Gunther, H. Hubel, A. Kluge, K. Krien, H. Toschinski, Nuclear Phys. A123, 386 (1969).

16. T. Sundstrom, P. Sparrman, J. O. Lindstrom, and J. Lindskog, Arkiv Fysik 26, 377 (1964).

17. Nuclear Data Sheets 10, 359 (1973).

18. S. Koicki, J. Simic, and A. Kukoc, Nuclear Phys. 10, 412 (1959).

19. Z. Grabowski, J. E. Thun, M. S. El-Nesr, and W. D. Hamilton, Z. Physik 167, 111 (1962).

20. S. Koicki, A. Koicki, G. T. Wood, and M. E. Caspari, Phys. Rev. 143, 148 (1966).

21. A. J. Becker and R. M. Steffen, Bull. Am. Phys. Soc. 12, No. 5, 715, FE8 (1967).

22. E. N. Kaufmann, J. D. Bowman, and S. K. Bhattacherjee, Nuclear Phys. A119, 417 (1968).

23. R. Beraud, I. Berkes, J. Daniere, R. Haroutunian, G. Marest, and R. Rougny, J. Phys. (Paris) 31, 1025 (1970).

24. J. D. Bowman, J. DeBoer, and F. Boehm, Nuclear Phys. 61, 682 (1965).

25. A. P. Agnihotry, K. P. Gopinathan, H. C. Jain, and C. V. K. Baba, Phys. Rev. C6, 321 (1972).

26. C. M. Lederer, J. M. Hollander, and I. Perlman, Table of Isotopes (6th ed.), John Wiley & Sons, Inc., New York (1967).

27. A. M. Feingold and S. Frankel, Phys. Rev. 97, 1025 (1955).

28. L. C. Biedenharn and M. E. Rose, Phys. Rev. 134, B8 (1964).

29. E. V. Ivash, Nuovo Cimento 9, 136 (1958).

30. M. A. Listengarten, I. M. Band, E. F. Zganjar, and J. H. Hamilton, L Shell Particle Parameters for Angular Correlations of Conversion Electrons, in Internal Conversion Processes (ed. J. H. Hamilton), (App. 2), Academic Press, New York (1966).

31. P. R. Bevington, Data Reduction and Error Analysis for the Physical Sciences, McGraw-Hill, New York (1969).

32. M. E. Rose, Phys. Rev. 91, 610 (1953).

33. D. C. Camp and A. L. Van Lehn, Nucl. Instr. and Meth. 76, 192 (1969).

34. D. C. Camp and A. L. Van Lehn, Nucl. Instr. and Meth. 87, 147 (1970).

VITA

Craig McKinney Hill was born on May 25, 1942, in Atlanta, Georgia. He received his elementary and secondary education in the Atlanta public schools. Following four years of service in the U. S. Marine Corps, he returned to Georgia Tech to complete his undergraduate studies. He was elected to membership in Phi Kappa Phi honor society in 1967, and received the B. S. degree in Physics, with honor, in June of 1968. One year later he obtained the M. S. degree in Physics from Georgia Tech. He was the recipient of a three-year NDEA graduate fellowship, and held a teaching assistantship in the School of Physics.